

Bone marrow remodeling supports hematopoiesis in response to immune thrombocytopenia progression in mice

Oliver J. Herd,¹ Gulab Fatima Rani,¹ James P. Hewitson,¹ Karen Hogg,² Andrew P. Stone,¹ Nichola Cooper,³ David G. Kent,¹ Paul G. Genever,¹ and Ian S. Hitchcock¹

¹York Biomedical Research Institute; ²Technology Facility, Department of Biology, University of York, York, United Kingdom; and ³Centre for Haematology, Department of Immunology and Inflammation and Department of Medicine, Hammersmith Hospital, Imperial College London, London, United Kingdom

Key Points

- Sustained ITP activates and increases the number of functional LT-HSCs.
- The remodeled ITP bone marrow enhances hematopoiesis.

Immune thrombocytopenia (ITP) is an acquired autoimmune condition characterized by both reduced platelet production and the destruction of functionally normal platelets by sustained attack from the immune system. However, the effect of prolonged ITP on the more immature hematopoietic progenitors remains an open area of investigation. By using a murine *in vivo* model of extended ITP, we revealed that ITP progression drives considerable progenitor expansion and bone marrow (BM) remodeling. Single-cell assays using Lin⁻Sca1⁺c-Kit⁺CD48⁻CD150⁺ long-term hematopoietic stem cells (LT-HSCs) revealed elevated LT-HSC activation and proliferation *in vitro*. However, the increased activation did not come at the expense of LT-HSC functionality as measured by *in vivo* serial transplantations. ITP progression was associated with considerable BM vasodilation and angiogenesis, as well as a twofold increase in the local production of CXCL12, a cytokine essential for LT-HSC function and BM homing expressed at high levels by LepR⁺ BM stromal cells. This was associated with a 1.5-fold increase in LepR⁺ BM stromal cells and a 5.5-fold improvement in progenitor homing to the BM. The increase in stromal cells was transient and reverted back to baseline after platelet count returned to normal, but the vasculature changes in the BM persisted. Together, our data demonstrate that LT-HSCs expand in response to ITP and that LT-HSC functionality during sustained hematopoietic stress is maintained through an adapting BM microenvironment.

Introduction

Increased destruction and decreased production of functionally normal platelets is a hallmark of immune thrombocytopenia (ITP), which manifests as a bleeding tendency.¹⁻³ The majority of patients with ITP develop serum platelet-specific autoantibodies that target platelets for destruction and are primarily against platelet glycoprotein IIb and IIIa (GPIIb/GPIIIa) (CD41/CD61), GPIb/GPIX (CD42c/CD42a), GPV (CD42d), and GPIa/GPIIa (CD49b).⁴⁻⁷ Of these, autoantibodies against CD41 and CD61 are the most common.^{6,7} The spleen is the major site of platelet clearance, which is primarily mediated through phagocytosis by splenic macrophages or dendritic cells.^{8,9} ITP patients can be classified as newly diagnosed (<3 months) or persistent (<12 months), which is more common in children, as well as chronic (>12 months), which is more common in adults.^{10,11}

Submitted 24 November 2020; accepted 10 March 2021; prepublished online on *Blood Advances* First Edition 24 August 2021; final version published online 24 November 2021. DOI 10.1182/bloodadvances.2020003887.

For original data, please contact Ian S. Hitchcock via e-mail at ian.hitchcock@york.ac.uk. The full-text version of this article contains a data supplement.

© 2021 by The American Society of Hematology. Licensed under Creative Commons Attribution-NonCommercial-NoDerivatives 4.0 International (CC BY-NC-ND 4.0), permitting only noncommercial, nonderivative use with attribution. All other rights reserved.

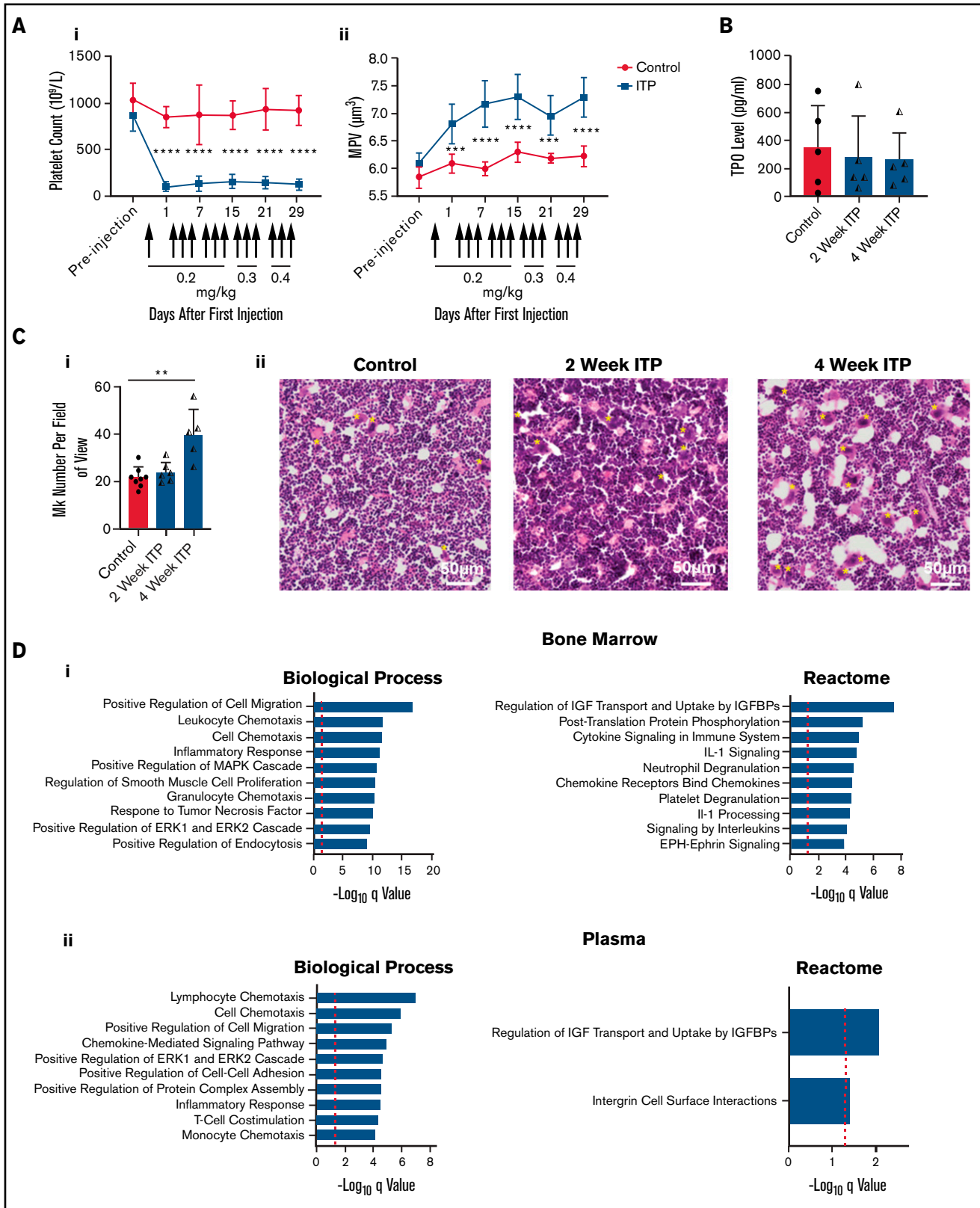


Figure 1. Repeated intraperitoneal injection of mice is a model for sustained ITP. (A) A single intraperitoneal injection of anti-CD41 antibody (delineated by an arrow) every 48 hours induces severe thrombocytopenia associated with an increase in mean platelet volume (MPV). For routine monitoring of ITP induction, mice were bled 24 hours after injection ($n = 5-10$ mice). P values were calculated by a two-way analysis of variance (ANOVA) with Sidak's multiple comparison test (**** $P < .0001$, MPV 1 day post injection control vs ITP *** $P = .0009$, MPV 21 days post injection control vs ITP *** $P = .0003$). (B) Circulating TPO levels during ITP progression ($n = 4-5$ mice; data are representative of 2 independent experiments). P values were calculated by a Kruskal-Wallis test with Dunn's multiple comparisons test (control vs 2-week ITP $P > .99$,

During conditions of chronic hematopoietic stress, such as infection and inflammation, hematopoietic stem cells (HSCs) are activated to meet the increased demand in blood cell production.^{12,13} Exit from quiescence has been previously associated with a loss in regenerative capacity and may eventually cause pancytopenia.¹⁴⁻¹⁶ During ITP, the requirement for HSC differentiation is twofold. First, the increased platelet demand caused by autoimmune-mediated platelet destruction drives megakaryopoiesis.¹⁷⁻²⁰ Second, sustained immune system activation that drives platelet destruction requires replenishment from progenitors.^{12,13,21} Despite this, there have been no reports of HSC exhaustion or pancytopenia in patients with chronic ITP, suggesting that HSCs may receive additional support.

Recent evidence shows that the bone marrow (BM) microenvironment provides supportive rather than instructive input for HSC differentiation.²² Furthermore, the microenvironment is pliable and can contribute to disease progression by driving the expression of proliferative or proinflammatory factors or by downregulating factors that traditionally support HSC function. Such changes may be induced by the presence of infection,^{23,24} the development of malignancy,^{25,26} or the administration of drugs.²⁷ Whether the BM microenvironment actively remodels itself in response to various chemical or cellular insults to resolve and/or minimize hematopoietic stress remains unclear.

Antibody-mediated platelet destruction can be recreated *in vivo* by administering anti-platelet antibodies to cause thrombocytopenia.²⁸ This is known as the passive transfer model of ITP, and its historical use has been in the form of a single injection^{29,30} or multiple injections of anti-platelet antibodies spanning 1 to 2 weeks.³¹⁻³⁵ To better model sustained ITP, we extend this model to 4 weeks, showing that the increased demand on hematopoiesis is met by an increase in the number of functional HSCs. We hypothesize that this is achieved through an interactive and iterative relationship between differentiating HSCs and an adapting supportive BM microenvironment in an effort to maintain homeostasis.

Methods

Mice

Mice used in this study were female wild-type (WT) C57BL/6J (B6) (CD45.1) or CD45.2 mice unless otherwise stated. *Cxcl12*^{DsRed/+} knock-in mice were previously bred onto a B6 genetic background and were generated by recombining *DsRed-Express2* into the endogenous *Cxcl12* locus as previously described.³⁶ The WT and *Cxcl12*^{DsRed/+} mice used for this study were between 8 and 12 weeks old. Female B6^{W41/W41} CD45.1 mice 7 to 9 months old were used as recipients for low-dose Lin⁻Sca1⁺c-Kit⁺CD48⁻CD150⁺ long-term hematopoietic stem cell (LT-HSC) transplantation experiments. All mice were bred and housed under specified pathogen-free conditions. All animal procedures were approved by the University of York Animal Welfare and Ethical Review Board and carried out under United Kingdom Home Office license

(PPL P24552FC1). Animals were euthanized by CO₂ asphyxia and cervical dislocation or overdose of anesthesia and exsanguination. Mice were randomly allocated to the immunoglobulin G (IgG) or anti-CD41 group, and downstream sample analysis was performed in a blinded manner. Primers for genotyping of the *Cxcl12*^{DsRed} allele were 5'-AAGAAGCCCGTGAAGCTGC-3' and 5'-TCCTCGTTGTGGGAGGTGAT-3'.

Passive ITP model

Mice were administered anti-mouse CD41 antibody (clone MWReg30; BD Pharmingen) to selectively deplete platelets or IgG1 (to act as a control) via intraperitoneal injection every 48 hours for up to 4 weeks (duration was dependent on the experiment). Concentration of anti-CD41 or IgG1 ranged between 0.2 and 0.4 mg/kg as indicated in Figure 1. As described previously, antibody dose escalation was necessary to maintain thrombocytopenia over time.³⁴ In our study, 0.2 mg/kg anti-CD41 was sufficient to maintain thrombocytopenia for the first 2 weeks, followed by an increase of 0.1 mg/kg per week thereafter.

Competitive transplantation assay

WT (CD45.2) donor mice were injected with anti-mouse CD41 antibody, whereas WT (CD45.1) donor mice were injected with IgG1 for 4 weeks (as described above). CD45.1 recipient mice were administered total body gamma radiation with 2 doses of 5.5 Gy 24 hours apart (lethal irradiation). For primary transplants, flushed BM from donor mice was prepared by mixing CD45.1 and CD45.2 BM cells in a 3:1, 1:1, or 1:3 ratio and resuspending them in sterile phosphate-buffered saline (PBS). A total of 5 × 10⁶ cells in a final volume of 200 μL was injected into the tail vein of each of the recipient mice. For secondary transplants, 2 × 10⁷ BM cells from primary transplant donors (pooled within each group) were further transplanted into CD45.1 recipient mice. All recipient mice were administered oral antibiotic Baytril (Bayer, Leverkusen, Germany) in drinking water for 14 days post-transplantation as a prophylactic treatment against bacterial infection. Recipient mice were bled at 4, 8, 12, 16, and 20 weeks to monitor donor chimerism and relative mature cell production by flow cytometry. Full details of antibodies used and flow cytometry methodology are available in the Supplemental Material.

Cell sorting and transplantation experiments

Lin⁻ donor cells were immunomagnetically enriched before cell sorting based upon the negative expression of lineage markers via the Easy-Sep Mouse Hematopoietic Progenitor Cell Isolation Kit (19856, STEMCELL Technologies) according to the manufacturer's instructions. After enrichment, cells were stained for progenitor markers as described in the Supplemental Material.

For homing assays, ~15 000 Lin⁻Sca1⁺c-Kit⁺ (LSK) cells from naïve CD45.1 mice were administered in 100 μL sterile PBS per recipient mouse via tail vein injection. Recipient mice were lethally irradiated CD45.2 mice that had previously been administered anti-CD41 or

Figure 1 (continued) control vs 4-week ITP $P > .99$, 2-week ITP vs 4-week ITP $P > .99$. (Ci) BM megakaryocyte (Mk) numbers during ITP progression ($n = 5-8$ mice; data are representative of 2 independent experiments). P values were calculated by a Kruskal-Wallis test with Dunn's multiple comparisons test (control vs 2-week ITP $P > .99$, control vs 4-week ITP $**P = .0069$, 2-week ITP vs 4-week ITP $P = .10$). (Cii) Representative hematoxylin and eosin stained diaphysis BM sections from WT femurs with Mk's indicated by yellow stars. Images were obtained using a Zeiss AxioScan.Z1 slide scanner. (D) Gene Ontology terms within the biological process domain and reactome pathways identified by STRING analysis of upregulated cytokines in the BM (i) and plasma (ii) of mice with 4-week ITP relative to control. Cytokine analysis was performed using a Proteome Profiler Mouse XL Cytokine Array Kit (R&D Systems). Data are shown as mean ± standard deviation (SD). Red dotted lines, $\log_{10}(0.05) = 1.3$; EPH, Erythropoietin producing hepatocellular carcinoma receptors; Ephrin=EPH receptors interacting proteins; IL-1, interleukin-1.

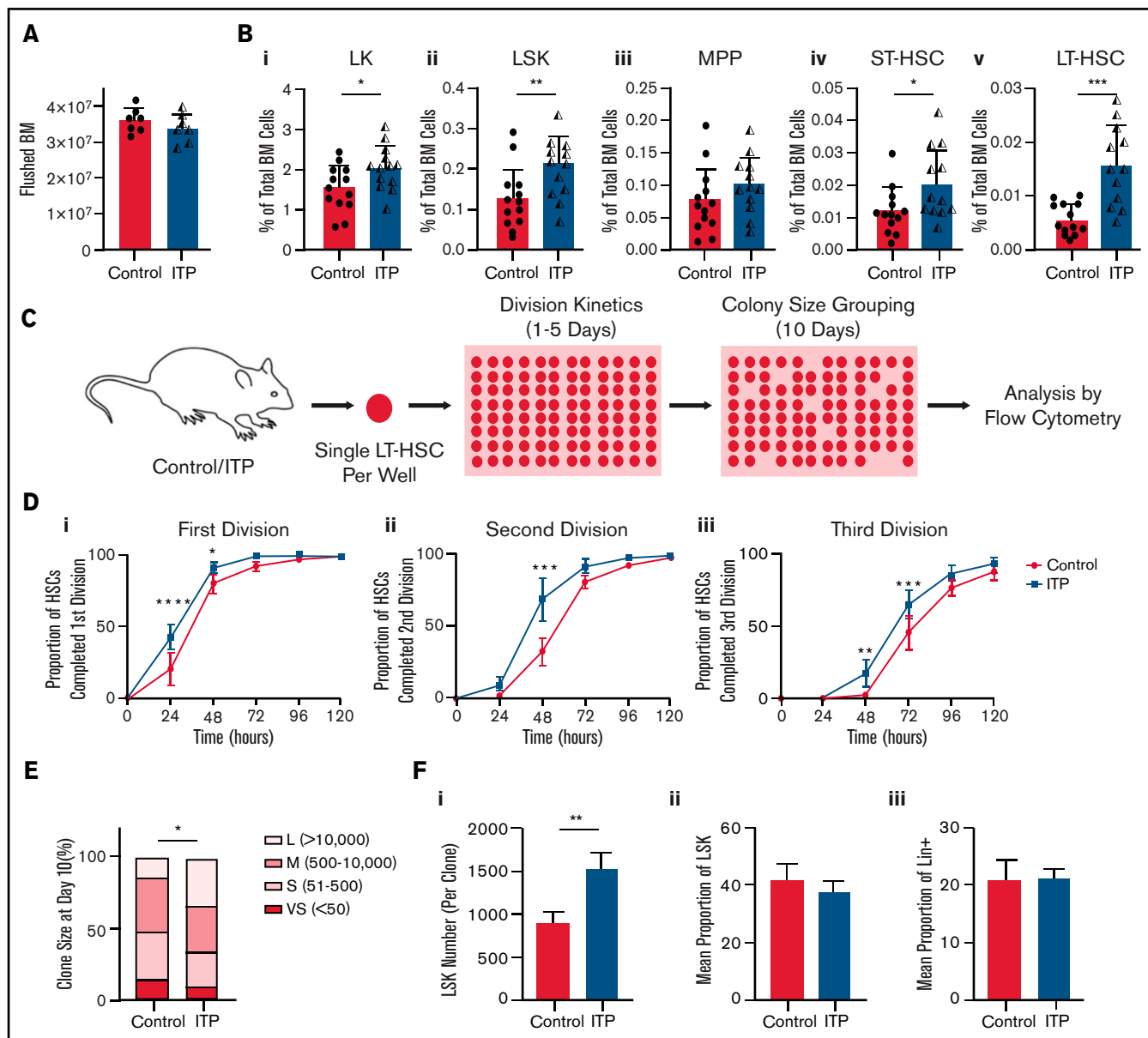


Figure 2. Sustained ITP drives progenitor expansion and LT-HSC proliferation. (A) Total cell counts from flushed BM ($n = 7$; data are representative of 2 independent experiments; Mann-Whitney U test $P = .46$). (B) Flow cytometry analysis of hematopoietic progenitor populations ($n = 13$; data are representative of 3 independent experiments): (i) $\text{Lin}^- \text{c-Kit}^+$ (LK) $^*P = .034$, (ii) $\text{Lin}^- \text{Sca}^{-1} \text{c-Kit}^+$ (LSK) $^{**}P = .0055$, (iii) $\text{LSK CD48}^+ \text{CD150}^-$ $P = .068$, (iv) $\text{LSK CD48}^- \text{CD150}^-$ $^*P = .019$, (v) $\text{LSK CD48}^- \text{CD150}^+$ $^{***}P = .0005$. P values were calculated by Mann-Whitney U tests. (C) Experimental outline for C-E. (D) Cumulative time taken for a single LT-HSC to complete first (i), second (ii), and third (iii) division ($n = 4$ -5 mice; data are representative of 2 independent experiments). P values were calculated by a two-way ANOVA with Sidak's multiple comparison test. (E) Colony size after 10 days in culture ($n = 3$ -4 mice; data are representative of 2 independent experiments). $^*P = .020$, calculated by a two-way ANOVA. Colonies were categorized as very small (VS; <50), small (S; 51-500), medium (M; 501-10 000), or large (L; >10 000). (F) After 10 days in culture, colonies were analyzed by flow cytometry for the expression of lineage and LSK markers ($n = 143$ clones from controls and $n = 208$ clones from mice with sustained ITP; $n = 3$ mice; data are representative of 2 independent experiments). LSK numbers (i, $^{**}P = .006$), LSK frequency (ii, $P = .92$), and Lin^+ cell frequency (iii, $P = .55$). P values were calculated by Mann-Whitney U tests. All data are shown as mean \pm SD except in panel E, which shows mean \pm standard error of the mean (SEM). MPP, multipotent progenitors; ST-HSC, short-term LT-HSC.

IgG for 4 weeks. After 36 hours, BM was harvested and stained for donor cells followed by flow cytometry analysis as described in the Supplemental Material.

For low-dose HSC transplantation experiments, 100 LT-HSCs from 4-week-old CD45.2 mice injected with either anti-CD41 or IgG were

bulk sorted into 1 mL of PBS and diluted so that each sublethally irradiated (1 dose of 3.6 Gy) $\text{B6}^{\text{W}41/\text{W}41} \text{CD45.1}$ mouse received either 10 or 3 LT-HSCs. Recipient $\text{B6}^{\text{W}41/\text{W}41} \text{CD45.1}$ mice were bled at 4, 8, or 11 weeks post-transplantation, and peripheral blood was analyzed to determine levels of chimerism as described in the supplemental Material. The experiment was terminated at 11 weeks because of

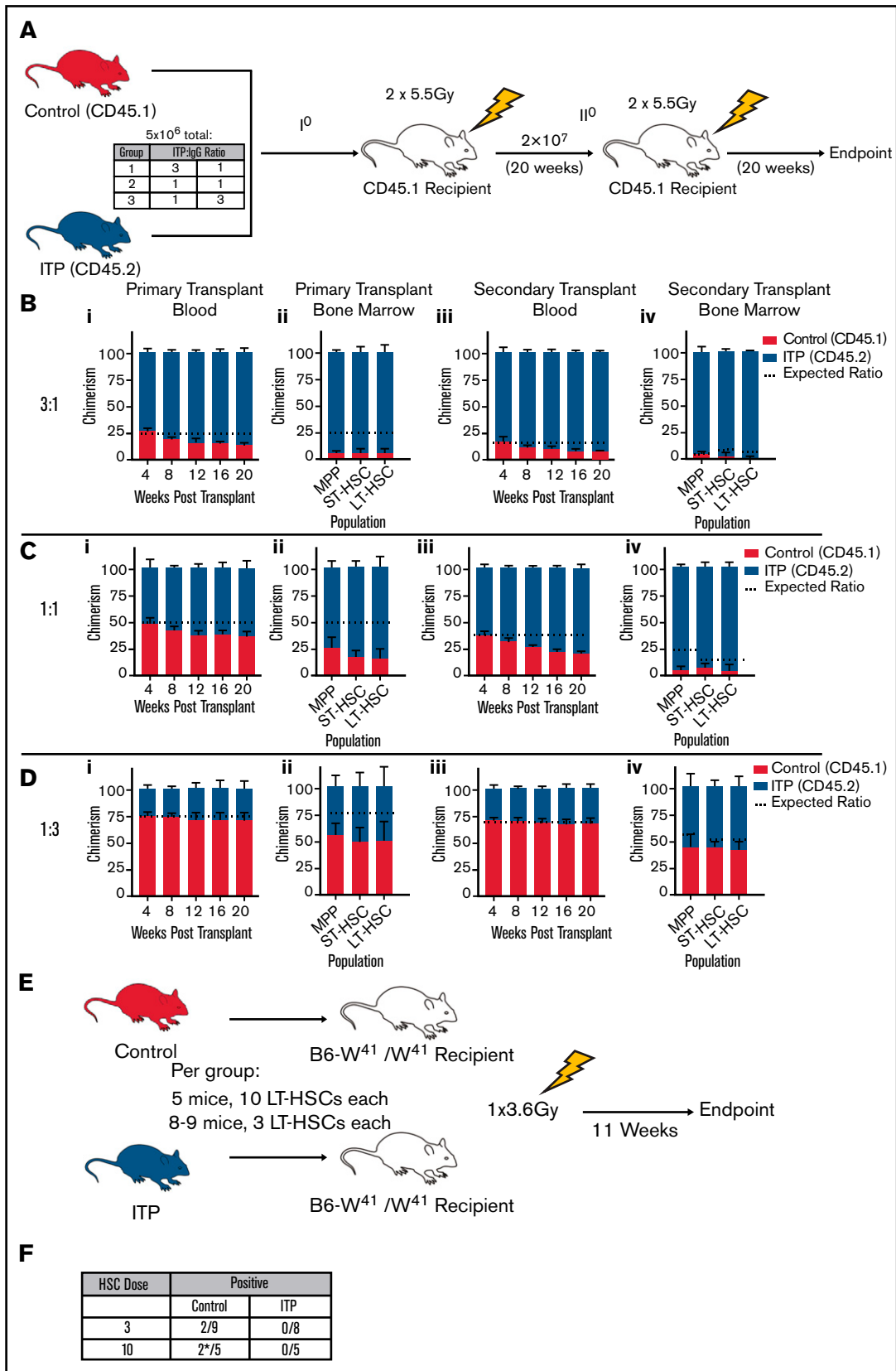


Figure 3. Sustained ITP increases the frequency of functional LT-HSCs in vivo. (A) Experimental outline for B-D. (B, C, D) Peripheral blood from primary recipients 4 to 20 weeks after transplantation. (Bii, Cii, Dii) Analysis of BM from primary recipients 20 weeks after transplantation. (Biii, Ciii, Diii) Analysis of peripheral blood from secondary

COVID-19 restrictions; therefore, it was not possible to confirm whether mice with <1% chimerism (trace chimerism) would progress to develop >1% chimerism with time. Mice with trace chimerism are highlighted in "Results." For in vitro LT-HSC assays, 1 LT-HSC was sorted per well of a round-bottom 96-well plate, with each well containing 50 μ L of LT-HSC media as described in the supplemental Material. Cells were sorted by using a 4-laser Beckman Coulter Astrios EQ sorter.

Statistical analysis

Statistical analyses were performed using GraphPad Prism software (Version 8.4.3). In statistical graphs, data points indicate individual samples, and nonsignificant values ($P > .05$) are not shown. P values are provided in the figure legends.

Results

ITP progression drives hematopoietic progenitor expansion

To determine the long-term impact of ITP on hematopoiesis, a model for sustained ITP was established by repeated (every 48 hours) intraperitoneal injection of mice with a monoclonal rat anti-mouse CD41 antibody or rat IgG1 isotype control for a period of 4 weeks (Figure 1). From 2 weeks, increased doses of rat anti-CD41 antibody were necessary to maintain thrombocytopenia, presumably to counteract compensatory thrombopoiesis³⁴ and/or antibody generation against the injected rat IgG1 antibody. Hereafter, mice treated with anti-CD41 are referred to as the ITP group, and mice treated with IgG1 are referred to as the control group.

This passive transfer model maintains severe thrombocytopenia (defined here as a mean platelet count below $200 \times 10^9/L$) from a mean resting platelet count of $865 \times 10^9/L$. Mice in the ITP group had a platelet count ranging from $57 \times 10^9/L$ to $327 \times 10^9/L$, and controls had a platelet count ranging from $584 \times 10^9/L$ to $1402 \times 10^9/L$. In addition, mice with ITP had an increase in mean platelet volume, which indicated a higher platelet turnover (Figure 1Ai). Plasma thrombopoietin (TPO) levels were not affected by ITP, although an increase in the number of BM megakaryocytes was observed at later time points (Figure 1B-C). As inflammatory factors are known to drive emergency megakaryopoiesis independently of TPO,³⁷ the plasma and BM supernatant were analyzed. Biological processes involved in the inflammatory response and positive regulation of MAPK signaling (such as CCL21) were upregulated in both the plasma and the BM (Figure 1D; supplemental Figure 1). Upregulation of these biological processes was higher in the BM than in the plasma, which was of interest because inflammation and MAPK signaling have previously been shown to affect LT-HSC quiescence and function.^{37,38} In addition, some biological processes and reactome pathways have also been shown to affect LT-HSC quiescence and function; interleukin-1 signaling and smooth muscle cell proliferation (VEGF, MMP2,

WISP1, and IGFBP-3) were uniquely upregulated in the BM (Figure 1D; supplemental Figure 1).³⁹⁻⁴³

To test whether sustained ITP affects hematopoietic progenitors, mice in the ITP group and controls were compared by flow cytometry. ITP had no effect on total BM cellularity (Figure 2A), but caused a 1.3-fold expansion in the percentage of BM-derived Lin⁻Sca1⁻c-Kit⁺ (LK cells, enriched for myeloid progenitors) and a 1.7-fold expansion in LSK cells, which are enriched for HSCs (Figure 2Bi-ii). Progenitor expansion in the spleen was also observed (supplemental Figure 2C-E), with a twofold expansion in the LK population and a 2.9-fold expansion in the LSK population, suggesting the presence of extramedullary hematopoiesis in ITP. The LSK population was subdivided further using signaling lymphocyte activation molecule (SLAM) markers,⁴⁴ with the largest expansion in the LT-HSC fraction (2.8-fold in the BM and 9.7-fold in the spleen) (Figure 2Bv). Gating strategies of analyzed BM and splenic populations are shown in supplemental Figure 2A-B.

To determine the functional effect of ITP on LT-HSCs, single LT-HSCs from mice in the ITP group or controls were isolated and cultured in conditions that maintain LT-HSC activity (Figure 2C) and were analyzed for changes in cell division, colony size, and cell phenotype.^{45,46} LT-HSCs from mice with ITP proliferated faster and took less time to complete first, second, and third divisions (Figure 2D). This faster division formed larger colonies at day 10 of culture (Figure 2E), which was driven by an increase in LSK progenitors (Figure 2Fi). However, despite the overall increase in number of cells per clone, ITP did not alter the proportion of differentiated and stem or progenitor cells within clones, suggesting that progenitor expansion was not accompanied by differentiation or self-renewal defects (Figure 2Fii-iii). Our results indicate that sustained ITP induces the cycling of phenotypic LT-HSCs, causing an expansion of hematopoietic progenitors without compromising LT-HSC function.

Sustained ITP increases the number of functional LT-HSCs

To assess the in vivo functional capacity of the expanded progenitor compartment, competitive transplantation assays were performed using 5×10^6 whole BM cells from ITP and control donors in 3:1, 1:1, and 1:3 ratios (Figure 3A). This was followed by secondary transplantations after 20 weeks using 2×10^7 pooled whole BM cells from mice within each ratio group. In the 1:1 group (Figure 3C), the contribution of ITP donors to peripheral chimerism increased to $63\% \pm 6\%$ (mean \pm standard deviation), accompanied by an expanded contribution to the BM LT-HSC phenotype at $85\% \pm 10\%$. Secondary transplantation data similarly showed an increased contribution by donor cells derived from the ITP group to mature cell production. Together, these transplantation data demonstrate the existence of an expanded, self-renewing pool of functional LT-HSCs in the BM of mice with sustained ITP.

Figure 3 (continued) recipients 4 to 20 weeks after transplantation. (Biv, Civ, Div) Analysis of BM from secondary recipients 20 weeks after transplantation. The horizontal dotted line shows the expected ratio if ITP had no effect on chimerism; for primary recipients, this was calculated on the basis of the transplanted ratio of donor cells, and for secondary recipients, this was calculated on the basis of the end point of the primary recipients ($n = 5$ mice per recipient group). (E) Experimental outline for panel F. (F) After 11 weeks, 2 of 9 recipients receiving 3 control LT-HSCs and 2 of 5 recipients receiving 10 LT-HSCs experienced chimerism, whereas 0 recipients receiving ITP LT-HSCs experienced chimerism ($P = .013$). P value was calculated with a χ^2 test. A successful transplantation was defined as >1% CD45.2 chimerism. After 11 weeks, 1 mouse transplanted with 10 control LT-HSCs showed >1% CD45.2 chimerism, and 1 mouse showed trace amounts of chimerism (<1%) as marked by an asterisk (*). All data are shown as mean \pm SD.

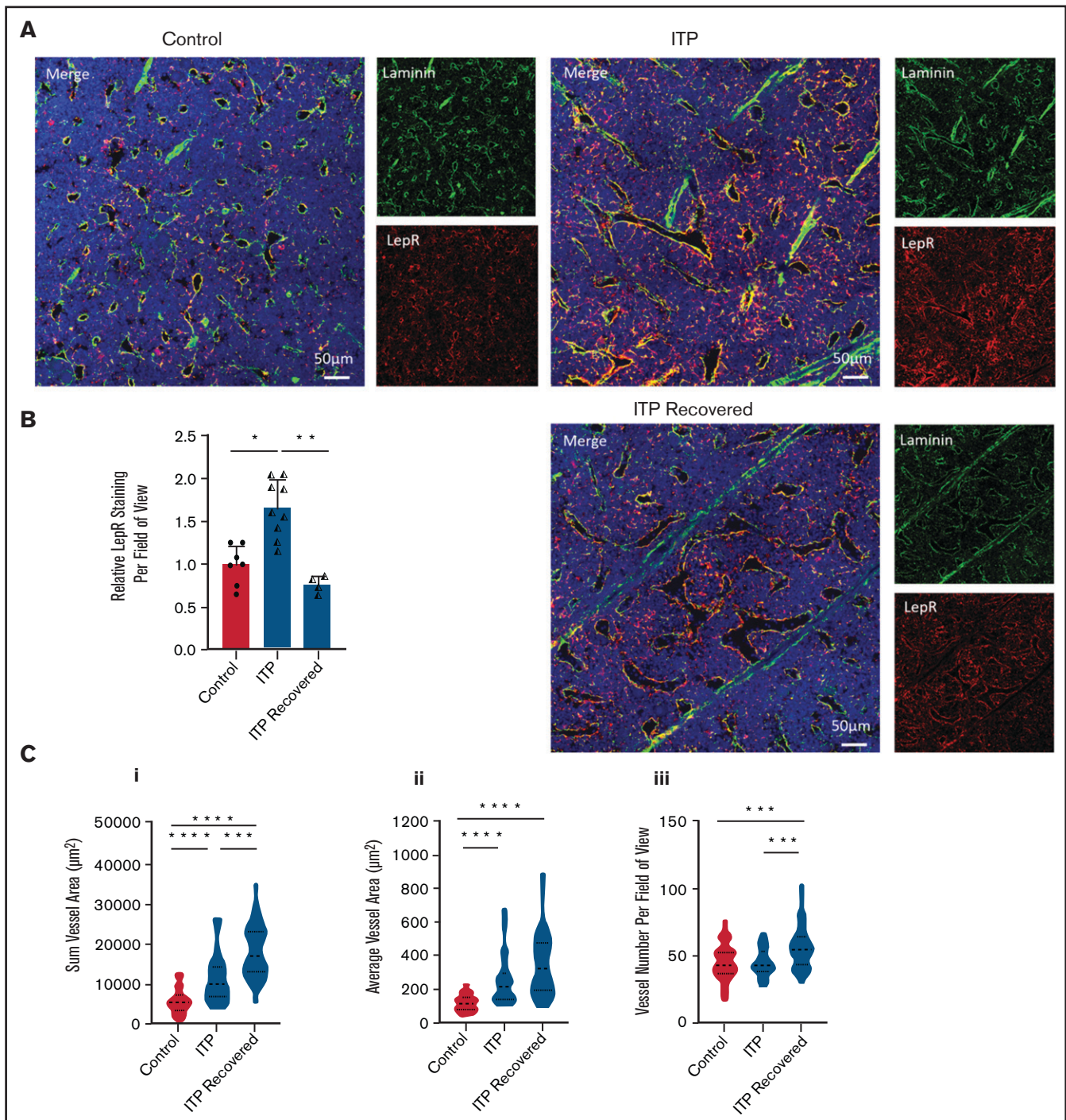


Figure 4. Sustained ITP remodels the BM microenvironment. ITP progression was associated with blood vessel structural changes and reversible changes in stromal cell number. Mice were treated with IgG (control) or anti-CD41 (ITP) for 4 weeks. An additional group of ITP mice were allowed to recover for an additional 4 weeks after the last injection of anti-CD41, during which platelet count returned to normal by day 18 (ITP recovered group). All data shown from controls and mice with ITP are representative of 3 independent experiments; the data from ITP recovered mice is representative of 1 independent experiment. (A) Representative confocal images of control, ITP, and ITP recovered diaphysis BM from WT femurs. (B) Relative numbers of LepR⁺ stromal cells were inferred by comparing total LepR staining between groups. Staining was quantified by exporting the LepR channel images as TIFF images and quantifying total staining relative to controls using ImageJ software (n = 4-9 mice; data are mean ± SD, with an average of 10 images analyzed per mouse). Control vs ITP **P* = .018, control vs ITP recovered *P* = .91, ITP vs ITP recovered ***P* = .0021. *P* values were calculated by using a Kruskal-Wallis test with Dunn's multiple comparison test. (C) Vessel analysis showing (i) sum vessel area (control vs ITP *****P* < .0001, control vs ITP recovered *****P* < .0001, ITP vs ITP recovered ****P* = .0001), (ii) average vessel area (control vs ITP *****P* < .0001, control vs ITP recovered *****P* < .0001, ITP vs ITP recovered *P* = .066), and (iii) vessel number (control vs ITP *P* > .99, control vs ITP recovered ****P* = .0008, ITP vs ITP recovered ****P* = .0007). Vessel information was quantified using StrataQuest analysis software (TissueGnostics). *P* values were calculated by a Kruskal-Wallis test with Dunn's multiple comparison test (n = 44-55 images). Violin plots show median values and upper and lower quartiles, with an average of 10 images analyzed per mouse. All data are shown as mean ± SD.

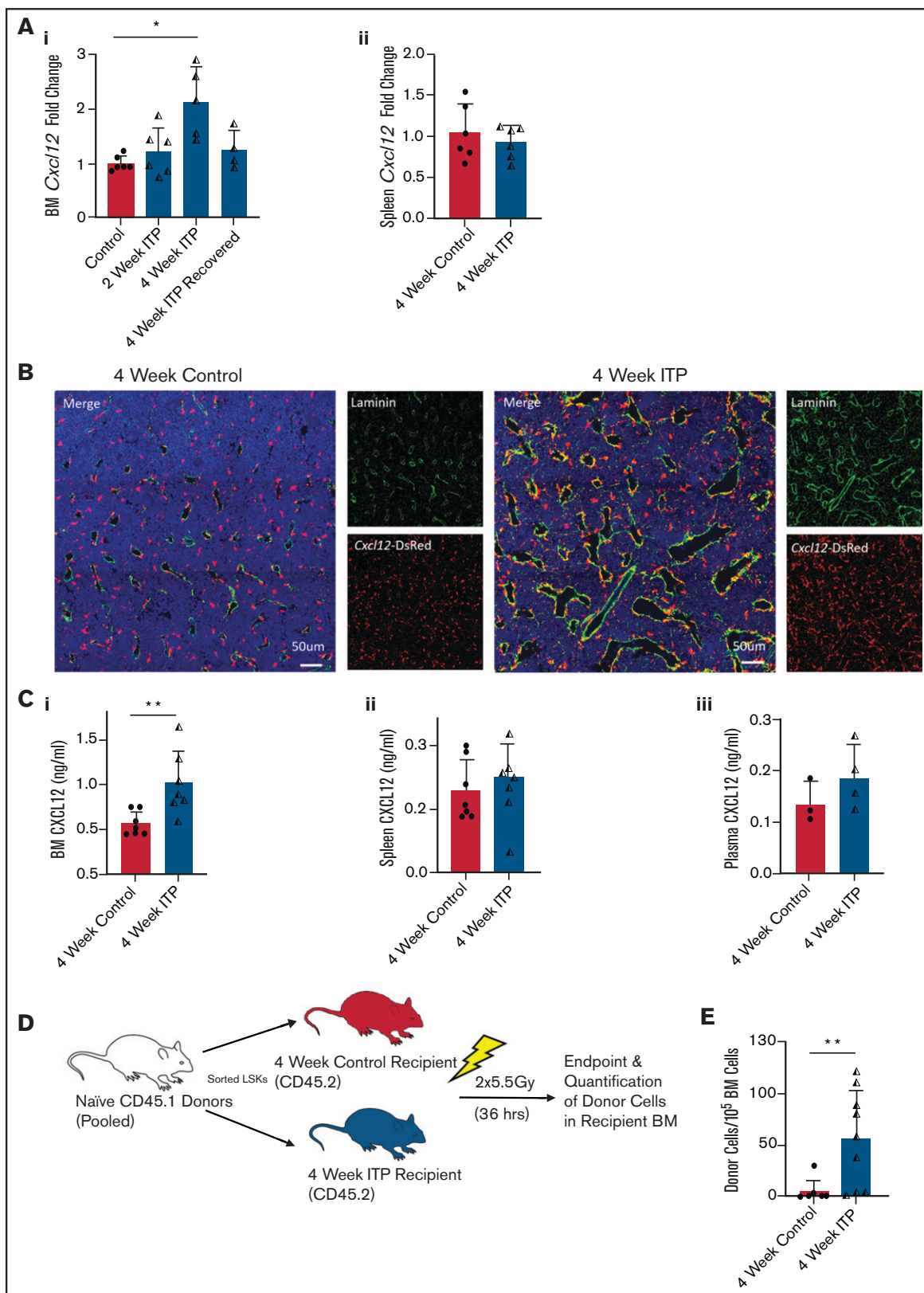


Figure 5. ITP progression increases BM CXCL12 expression and is associated with increased progenitor homing. (Ai) BM *Cxcl12* expression (n = 4-6 mice; data are representative of 1-2 independent experiments) (control vs 2-week ITP $P > .99$, control vs 4-week ITP $*P = .021$, control vs 4-week ITP recovered $P > .99$, 2-week ITP vs 4-week ITP $P = .14$, 4-week ITP vs 4-week ITP recovered $P = .43$). P values were calculated by a Kruskal-Wallis test with Dunn's multiple comparison test. (Aii) Spleen *Cxcl12* expression (n = 6 mice; data are representative of 2 independent experiments; $P = .82$). P value was calculated by using a Mann-Whitney U test. (B) Representative confocal

To test LT-HSC functional capacity more directly, we next transplanted limiting numbers of highly purified LT-HSCs isolated using the Lin⁻Sca1⁺c-Kit⁺CD48⁻CD150⁺ phenotype. Either 3 or 10 LT-HSCs from the ITP or control groups were isolated and transplanted into sub-lethally irradiated B6^{W41/W41} CD45.1 mice (Figure 3E). Whereas 20% of mice receiving 3 LT-HSCs and 40% of mice receiving 10 LT-HSCs from the control group were positive, none of the mice receiving LT-HSCs from mice with ITP were repopulated (Figure 3F), suggesting that the LT-HSC phenotype in the ITP group does not contain as high a frequency of functional LT-HSCs.

ITP progression drives physical and biochemical changes within the BM HSC microenvironment

LT-HSC function is maintained through cytokine-cytokine receptor interactions and direct cell-cell contact between the LT-HSC and components of the perivascular BM microenvironment, including endothelial cells and LepR⁺ stromal cells.^{36,47,48} As sustained ITP causes expansion and functional changes in LT-HSCs, we next assessed whether this was accompanied by alterations in the BM microenvironment. Immunofluorescence microscopy identified significant changes in non-hematopoietic components of the HSC BM microenvironment, which were associated with ITP progression (Figure 4). Mice with 4-week ITP had a twofold increase in sum vessel area, which was attributed to an increase in average vessel area rather than any changes in vessel number. Effects were also observed at an earlier (2-week) time point, with a 1.5-fold increase in sum vessel area with no change in vessel number (supplemental Figure 3). Furthermore, at 4 weeks, there was a significant LepR⁺ stromal cell expansion (1.5-fold increase), but there were no changes in stromal cell number at 2 weeks.

To explore whether this remodeling of the BM microenvironment was reversible after recovery from thrombocytopenia, mice were allowed to recover for 4 weeks (ITP recovered group) before BM analysis (Figure 4). During this period of recovery, the platelet count reverted back to baseline by day 18 after the final anti-CD41 antibody injection (supplemental Figure 4). Despite the amelioration of thrombocytopenia, the substantial structural differences observed in the BM vasculature persisted with a further 1.5-fold increase in sum vessel area relative to the initial ITP group. In these mice, a significant increase in vessel number was observed as opposed to a further increase in average vessel area (Figure 4C). Conversely, numbers of LepR⁺ perivascular stromal cells reverted back to control levels, suggesting that stromal cell expansion was transient (Figure 4B).

Because perivascular LepR⁺ stromal cells are a major source of factors that influence LT-HSC function, including key microenvironment factors CXCL12, stem cell factor (SCF), and angiopoietin-1,^{36,47,49,50} and because they share the same microenvironment as LT-HSCs,^{47,51,52} we hypothesized that a transient increase in LepR⁺ stromal cells support LT-HSCs in response to sustained ITP. We measured the expression of *Cxcl12*, *Kitl*, and *Angpt1* in the BM and found that *Cxcl12* expression transiently increased to twofold levels in the ITP group (Figure 5A), but there were no significant changes in *Kitl* or *Angpt1*

(supplemental Figure 5B). Confocal imaging of the BM microenvironment from *Cxcl12*^{DsRed/+} reporter mice from an ITP group relative to a control group of mice revealed an increase in perivascular *Cxcl12* expression in mice from the ITP group (Figure 5B) and that this was driven by the expansion of LepR⁺ stromal cells (supplemental Figure 5A). CXCL12 levels were increased 1.8-fold in the BM supernatant of mice with ITP, but not in circulation or spleen, which confirms a BM-specific elevation in CXCL12 (Figure 5C). As CXCL12 has an essential role in progenitor homing to the BM,⁵³⁻⁵⁶ we hypothesized that mice with ITP would show an increased potential for progenitor homing (Figure 5D). Flow cytometry analysis of recipient BM revealed that naïve LSKs homed preferentially (5.5-fold increase) to the BM of irradiated mice with ITP relative to controls. Together, the data show that the BM actively remodels in response to ITP progression to create a site preferential for hematopoiesis. The expansion in LepR⁺ stromal cells and associated CXCL12 expression was transient, but vasculature changes persisted, the consequences of which are unknown.

Discussion

Although the mechanisms behind the development and maintenance of thrombocytopenia have been the subject of intensive research, the wider long-term effects of ITP progression are unclear. Here, we establish a model for investigating the effect of ITP progression on hematopoiesis and identify a significant expansion in phenotypic hematopoietic progenitors accompanied by a remodeling of the BM microenvironment. Functional assays demonstrated an increased proliferation and self-renewal potential of LT-HSCs and also indicated a shift in LT-HSC frequency within the LT-HSC phenotype. Assessment of the BM microenvironment identified alterations in key mediators of LT-HSC function, including an increase in total blood vessel area and a specific increase in LepR⁺ stromal cells. Together, these changes in LT-HSC activation and BM remodeling combine to counteract the stress of sustained ITP to ensure homeostasis within the hematopoietic system.

The murine ITP model we present shares a number of features with the clinical progression of chronic ITP, such as increased megakaryopoiesis while maintaining normal circulating TPO levels,^{17,19,20,57} which gives us confidence that our model was an appropriate choice for studying the effect of sustained ITP on hematopoiesis. Although increased megakaryopoiesis has been previously reported to occur as soon as 24 hours after anti-CD41 injection,⁵⁸ we did not observe increased megakaryopoiesis until after 4 weeks of injections. Cytokine analysis of BM and plasma samples at 4 weeks revealed an upregulation of proteins involved in the inflammatory response, which has been previously shown to drive megakaryopoiesis.³⁷ Because the cytokine signature in the ITP BM seemed to be more divergent from controls than the periphery, and that several upregulated biological processes and pathways have been previously shown to affect LT-HSC function,³⁸⁻⁴⁰ we asked whether sustained ITP may affect hematopoiesis more broadly.

The expansion in numbers of stem and progenitor cells in ITP in combination with the increase in proliferation observed in single LT-HSC in

Figure 5 (continued) images of diaphysis BM from femurs of *Cxcl12*^{DsRed/+} mice with sustained ITP vs controls. (C) CXCL12 enzyme-linked immunosorbent assay using (i) BM supernatant (n = 7 mice; **P = .0023), (ii) spleen homogenate (n = 7 mice; P = .38), and (iii) plasma (n = 3-4 mice; P = .23). Data are representative of 2 independent experiments. P values were calculated by using Mann-Whitney U tests. (D) Experimental outline for panel E. (E) Homing of naïve progenitors to the BM of mice with 4-week ITP vs controls (n = 8-9 mice; P = .004). Data are representative of 2 independent experiments. P value was calculated by using a Mann-Whitney U test. All data are mean ± SD.

vitro assays suggest that LT-HSCs might be activated in response to ITP. Competitive transplantation assays revealed that ITP drives an expansion of LT-HSCs with durable self-renewal, suggesting that this activation did not compromise LT-HSC activity. However, caution is needed when interpreting the relative numbers and activation status of LT-HSCs in diseased states. Whereas whole BM competitive transplants allow LT-HSC activity to be assessed in an unbiased fashion and indicate that numbers of functional LT-HSCs are increased, experiments assume that the expression of cell surface markers are not altered as a result of the experimental conditions. Indeed, it has been reported that during immune stimulation, BM cells have increased expression of Sca1 and CD150, causing non-HSC populations to appear in gates expected to be enriched in LT-HSC populations.⁵⁹ This can lead to dilution of experimental LT-HSCs vs control LT-HSCs when performing downstream experiments. Our low-dose LT-HSC transplantation experiments suggest that this may also occur in sustained ITP, in which sublethally irradiated mice that received LT-HSCs from ITP CD45.2 mice failed to repopulate compared with control CD45.2 mice. Together these data indicate that LT-HSCs might reside outside the traditional phenotype and that the LT-HSC phenotype is contaminated with a larger proportion of non-HSCs in an ITP setting.

It has recently been shown that progenitors activate and proliferate in response to acute antibody-mediated thrombocytopenia.³³ However, when ITP is extended to 2 weeks, LT-HSC functionality was impaired during serial transplants. This discrepancy with our results is potentially the result of differences in experimental setup. Ramasz et al³³ performed a primary competitive transplant using 300 LT-HSCs from mice with sustained ITP and 5×10^5 BM competitor cells from controls. After 16 weeks, they transplanted 300 ITP LT-HSCs from primary recipients into secondary recipients alongside 5×10^5 fresh BM competitor cells. The decreased contribution to peripheral blood reconstitution after each round of competitive transplant can be explained by our observation that the traditional LT-HSC phenotype is contaminated with a larger proportion of non-HSCs in ITP. However, when analyzing the LT-HSC pool as a whole (eg, using unbiased whole BM transplants), LT-HSC functionality is increased and preserves hematopoiesis in the long term.

The ability of LT-HSCs to maintain functionality under conditions of hematologic stress is essential for the preservation of hematopoiesis over the long term. When LT-HSCs are unable to meet the increased demand, such as in chronic infection^{23,24} or the development of malignancy,^{25,26} LT-HSCs exit quiescence and pancytopenia may arise. The increase in the functional LT-HSC pool in ITP therefore presents an intriguing dichotomy, and we studied the HSC BM microenvironment to determine whether beneficial changes in cell extrinsic factors may occur. ITP progression was associated with vasodilation and angiogenesis as well as LepR⁺ stromal cell expansion. The stromal cells maintained their classically defined perivascular location and therefore close or adjacent proximity to LT-HSCs,^{36,49,60} and their expansion was associated with an increase in CXCL12, which has a crucial role in maintaining LT-HSC function, including retention in the BM,^{36,54,55} repopulating activity,⁶¹ and quiescence.^{56,62} Furthermore, this increase in CXCL12 was BM specific and was expected to be primarily derived from LepR⁺ stromal cells,^{36,60} which we confirmed by confocal microscopy. Intriguingly, LepR⁺ stromal cell number reverted back to levels seen in control mice after recovery from

ITP, suggesting that thrombocytopenia may indirectly feed back to increase LT-HSC support during ITP progression.

The BM is the primary and preferential site for steady-state hematopoiesis in healthy adults, which is maintained by complex and multifactorial interactions from many different niche components.⁶³ Extramedullary hematopoiesis during infection or malignancy is often associated with loss of BM CXCL12 signaling.^{23,26,64-66} Our observation that ITP progression coincides with a transient increase in BM CXCL12 expression and associated increase in LT-HSC BM homing may be an important mechanism for maintaining LT-HSC functionality in conditions of elevated differentiation pressure, which is essential for maintenance of homeostasis long-term. As BM sinusoids are the preferred sites of progenitor homing as a result of low blood flow velocities and low wall shear rates,⁶⁷ it is possible that the increase in average vessel area in ITP could further reduce blood flow velocity and aid progenitor homing. As discussed, it has been shown that progenitors activate and proliferate in response to acute antibody-mediated thrombocytopenia, driven by the relocalization of SCF from the cytoplasm to the cell membrane of megakaryocytes.³³ Interestingly, this was not accompanied by an increase in total BM *Kitl* expression, suggesting that the proliferative effect on progenitors was post-transcriptionally regulated. In addition to its proliferative effects, SCF is essential for LT-HSC function.^{47,48} We have not assessed membrane-bound SCF expression in our model of sustained ITP, which may present a further mechanism that acts to preserve LT-HSC functionality during sustained ITP.

Our research therefore points to a concerted effort from various components of the BM microenvironment to create a nurturing environment maximizing megakaryopoiesis whilst minimizing LT-HSC exhaustion. BM examination is not routinely performed for chronic ITP patients¹⁰; thus, it is possible that significant changes in BM architecture can occur which requires further investigation. As we have tested only a single anti-CD41 antibody, it is important to investigate whether the effects on hematopoiesis and the BM microenvironment are comparable with other antiplatelet antibodies, such as anti-CD61 which are also common in ITP patients.^{6,7} Future studies should also address the effect of T-cell-mediated autoimmunity on hematopoiesis and the BM microenvironment, because our model of sustained ITP is T-cell independent. This is relevant because a minority of patients do not display autoantibodies, and in these patients, ITP is thought to be driven through cell-mediated autoimmunity.²¹

Acknowledgments

The authors thank the staff of the Biological Services Facility for animal husbandry, TissueGnostics application specialists and the staff of the Technological Facility Imaging and Cytometry Laboratory for assistance with flow cytometry and confocal microscopy, and Tess Stanley, Katuska Pulgar Prieto, and Maria Abril Arrendondo Garcia for experimental assistance.

This work was supported by funding from the White Rose Biotechnology and Biological Sciences Research Council Doctoral Training Partnership (BB/M011151/1) and the British Heart Foundation (PG/16/26/32099).

Authorship

Contribution: O.J.H. wrote the manuscript; O.J.H., I.S.H., and D.G.K. designed experiments; O.J.H. performed all experiments with assistance from G.F.R., J.P.H., K.H., A.P.S., D.G.K., and

I.S.H.; and all authors interpreted data and read and edited the final manuscript.

Conflict-of-interest disclosure: The authors declare no competing financial interests.

ORCID profiles: O.J.H., 0000-0003-0479-9342; G.F.R., 0000-0002-2209-1893; J.P.H., 0000-0002-3265-6763; K.H., 0000-

0001-7015-5102; A.P.S., 0000-0002-1087-9923; D.G.K., 0000-0001-7871-8811; I.S.H., 0000-0001-7170-6703

Correspondence: Ian S. Hitchcock, York Biomedical Research Institute and Department of Biology, University of York, Wentworth Way, York, YO10 5DD, United Kingdom; e-mail: ian.hitchcock@york.ac.uk.

References

1. Rodeghiero F, Stasi R, Gernsheimer T, et al. Standardization of terminology, definitions and outcome criteria in immune thrombocytopenic purpura of adults and children: report from an international working group. *Blood*. 2009;113(11):2386-2393.
2. Provan D, Stasi R, Newland AC, et al. International consensus report on the investigation and management of primary immune thrombocytopenia. *Blood*. 2010;115(2):168-186.
3. Neunert C, Lim W, Crowther M, Cohen A, Solberg L Jr, Crowther MA; American Society of Hematology. The American Society of Hematology 2011 evidence-based practice guideline for immune thrombocytopenia. *Blood*. 2011;117(16):4190-4207.
4. He R, Reid DM, Jones CE, Shulman NR. Spectrum of Ig classes, specificities, and titers of serum antiglycoproteins in chronic idiopathic thrombocytopenic purpura. *Blood*. 1994;83(4):1024-1032.
5. van Leeuwen EF, van der Ven JT, Engelfriet CP, von dem Borne AE. Specificity of autoantibodies in autoimmune thrombocytopenia. *Blood*. 1982;59(1):23-26.
6. Al-Samkari H, Rosovsky RP, Karp Leaf RS, et al. A modern reassessment of glycoprotein-specific direct platelet autoantibody testing in immune thrombocytopenia. *Blood Adv*. 2020;4(1):9-18.
7. Porcelijn L, Huiskes E, Oldert G, Schipperus M, Zwaginga JJ, de Haas M. Detection of platelet autoantibodies to identify immune thrombocytopenia: state of the art. *Br J Haematol*. 2018;182(3):423-426.
8. Najean Y, Rain JD, Billotey C. The site of destruction of autologous ¹¹¹In-labelled platelets and the efficiency of splenectomy in children and adults with idiopathic thrombocytopenic purpura: a study of 578 patients with 268 splenectomies. *Br J Haematol*. 1997;97(3):547-550.
9. Kuwana M, Okazaki Y, Ikeda Y. Splenic macrophages maintain the anti-platelet autoimmune response via uptake of opsonized platelets in patients with immune thrombocytopenic purpura. *J Thromb Haemost*. 2009;7(2):322-329.
10. Neunert C, Terrell DR, Arnold DM, et al. American Society of Hematology 2019 guidelines for immune thrombocytopenia. *Blood Adv*. 2019;3(23):3829-3866.
11. Moulis G, Sailler L, Lapeyre-Mestre M. Severe bleeding events in adults and children with primary immune thrombocytopenia: a systematic review: comment. *J Thromb Haemost*. 2015;13(8):1521-1522.
12. Takizawa H, Manz MG. Impact of inflammation on early hematopoiesis and the microenvironment. *Int J Hematol*. 2017;106(1):27-33.
13. Zhang CC. Hematopoietic stem cells: interplay with immunity. *Am J Blood Res*. 2012;2(4):219-227.
14. Baldridge MT, King KY, Boles NC, Weksberg DC, Goodell MA. Quiescent haematopoietic stem cells are activated by IFN-gamma in response to chronic infection. *Nature*. 2010;465(7299):793-797.
15. Essers MA, Offner S, Blanco-Bose WE, et al. IFNalpha activates dormant haematopoietic stem cells in vivo. *Nature*. 2009;458(7240):904-908.
16. Pinto AI, Brown N, Preham O, Doehl JSP, Ashwin H, Kaye PM. TNF signalling drives expansion of bone marrow CD4⁺ T cells responsible for HSC exhaustion in experimental visceral leishmaniasis. *PLoS Pathog*. 2017;13(7):e1006465.
17. Jubelirer SJ, Harpold R. The role of the bone marrow examination in the diagnosis of immune thrombocytopenic purpura: case series and literature review. *Clin Appl Thromb Hemost*. 2002;8(1):73-76.
18. Kuter DJ. The physiology of platelet production. *Stem Cells*. 1996;14(suppl 1):88-101.
19. Pisciotta AV, Stefanini M, Dameshek W. Studies on platelets. X. Morphologic characteristics of megakaryocytes by phase contrast microscopy in normals and in patients with idiopathic thrombocytopenic purpura. *Blood*. 1953;8(8):703-723.
20. Dameshek W, Miller EB. The megakaryocytes in idiopathic thrombocytopenic purpura, a form of hypersplenism. *Blood*. 1946;1(1):27-50.
21. Swinkels M, Rijkers M, Voorberg J, Vidarsson G, Leebeek FWG, Jansen AJG. Emerging concepts in immune thrombocytopenia. *Front Immunol*. 2018;9:880.
22. Yu VWC, Yusuf RZ, Oki T, et al. Epigenetic memory underlies cell-autonomous heterogeneous behavior of hematopoietic stem cells. *Cell*. 2016;167(5):1310-1322.e17.
23. Preham O, Pinho FA, Pinto AI, et al. CD4⁺ T cells alter the stromal microenvironment and repress medullary erythropoiesis in murine visceral leishmaniasis. *Front Immunol*. 2018;9(2958):2958.
24. Matatall KA, Jeong M, Chen S, et al. Chronic infection depletes hematopoietic stem cells through stress-induced terminal differentiation. *Cell Rep*. 2016;17(10):2584-2595.

25. Schmidt T, Kharabi Masouleh B, Loges S, et al. Loss or inhibition of stromal-derived PIGF prolongs survival of mice with imatinib-resistant Bcr-Abl1(+) leukemia. *Cancer Cell*. 2011;19(6):740-753.
26. Schepers K, Pietras EM, Reynaud D, et al. Myeloproliferative neoplasia remodels the endosteal bone marrow niche into a self-reinforcing leukemic niche. *Cell Stem Cell*. 2013;13(3):285-299.
27. Ghanima W, Geyer JT, Lee CS, et al. Bone marrow fibrosis in 66 patients with immune thrombocytopenia treated with thrombopoietin-receptor agonists: a single-center, long-term follow-up. *Haematologica*. 2014;99(5):937-944.
28. Semple JW. Animal models of immune thrombocytopenia (ITP). *Ann Hematol*. 2010;89(suppl 1):37-44.
29. Cox LH, Downs T, Dagg K, Henthorn J, Burstein SA. Interleukin-6 mRNA and protein increase in vivo following induction of acute thrombocytopenia in mice. *Blood*. 1991;77(2):286-293.
30. Siragam V, Crow AR, Brinc D, Song S, Freedman J, Lazarus AH. Intravenous immunoglobulin ameliorates ITP via activating Fc gamma receptors on dendritic cells. *Nat Med*. 2006;12(6):688-692.
31. Xiao J, Zhang C, Zhang Y, et al. Transplantation of adipose-derived mesenchymal stem cells into a murine model of passive chronic immune thrombocytopenia. *Transfusion*. 2012;52(12):2551-2558.
32. Morodomi Y, Kanaji S, Won E, Ruggeri ZM, Kanaji T. Mechanisms of anti-GPIIb α antibody-induced thrombocytopenia in mice. *Blood*. 2020;135(25):2292-2301.
33. Ramasz B, Krüger A, Reinhardt J, et al. Hematopoietic stem cell response to acute thrombocytopenia requires signaling through distinct receptor tyrosine kinases. *Blood*. 2019;134(13):1046-1058.
34. Katsman Y, Foo AH, Leontyev D, Branch DR. Improved mouse models for the study of treatment modalities for immune-mediated platelet destruction. *Transfusion*. 2010;50(6):1285-1294.
35. Neschadim A, Branch DR. Mouse models for immune-mediated platelet destruction or immune thrombocytopenia (ITP). *Curr Protoc Immunol*. 2016;113:15.30.1-15.30.13.
36. Ding L, Morrison SJ. Haematopoietic stem cells and early lymphoid progenitors occupy distinct bone marrow niches. *Nature*. 2013;495(7440):231-235.
37. Haas S, Hansson J, Klimmeck D, et al. Inflammation-induced emergency megakaryopoiesis driven by hematopoietic stem cell-like megakaryocyte progenitors. *Cell Stem Cell*. 2015;17(4):422-434.
38. Ramalingam P, Poulos MG, Lazzari E, et al. Chronic activation of endothelial MAPK disrupts hematopoiesis via NF κ B dependent inflammatory stress reversible by SCGF. *Nat Commun*. 2020;11(1):666.
39. Pietras EM, Mirantes-Barbeito C, Fong S, et al. Chronic interleukin-1 exposure drives haematopoietic stem cells towards precocious myeloid differentiation at the expense of self-renewal. *Nat Cell Biol*. 2016;18(6):607-618.
40. Kobayashi H, Butler JM, O'Donnell R, et al. Angiocrine factors from Akt-activated endothelial cells balance self-renewal and differentiation of haematopoietic stem cells. *Nat Cell Biol*. 2010;12(11):1046-1056.
41. Gerber HP, Malik AK, Solar GP, et al. VEGF regulates haematopoietic stem cell survival by an internal autocrine loop mechanism. *Nature*. 2002;417(6892):954-958.
42. Famili F, Brugman MH, Taskesen E, Naber BEA, Fodde R, Staal FJT. High levels of canonical Wnt signaling lead to loss of stemness and increased differentiation in hematopoietic stem cells. *Stem Cell Reports*. 2016;6(5):652-659.
43. Liu LQ, Sposato M, Liu HY, et al. Functional cloning of IGFBP-3 from human microvascular endothelial cells reveals its novel role in promoting proliferation of primitive CD34+CD38- hematopoietic cells in vitro. *Oncol Res*. 2003;13(6-10):359-371.
44. Kiel MJ, Yilmaz ÖH, Iwashita T, Yilmaz OH, Terhorst C, Morrison SJ. SLAM family receptors distinguish hematopoietic stem and progenitor cells and reveal endothelial niches for stem cells. *Cell*. 2005;121(7):1109-1121.
45. Kent DG, Dykstra BJ, Cheyne J, Ma E, Eaves CJ. Steel factor coordinately regulates the molecular signature and biologic function of hematopoietic stem cells. *Blood*. 2008;112(3):560-567.
46. Shepherd MS, Li J, Wilson NK, et al. Single-cell approaches identify the molecular network driving malignant hematopoietic stem cell self-renewal. *Blood*. 2018;132(8):791-803.
47. Ding L, Saunders TL, Enikolopov G, Morrison SJ. Endothelial and perivascular cells maintain haematopoietic stem cells. *Nature*. 2012;481(7382):457-462.
48. Barker JE. Sl/Slid hematopoietic progenitors are deficient in situ. *Exp Hematol*. 1994;22(2):174-177.
49. Asada N, Kunisaki Y, Pierce H, et al. Differential cytokine contributions of perivascular haematopoietic stem cell niches. *Nat Cell Biol*. 2017;19(3):214-223.
50. Baryawno N, Przybylski D, Kowalczyk MS, et al. A cellular taxonomy of the bone marrow stroma in homeostasis and leukemia. *Cell*. 2019;177(7):1915-1932.e16.
51. Acar M, Kocherlakota KS, Murphy MM, et al. Deep imaging of bone marrow shows non-dividing stem cells are mainly perisinusoidal. *Nature*. 2015;526(7571):126-130.
52. Kokkalis KD, Kunz L, Cabezas-Wallscheid N, et al. Adult blood stem cell localization reflects the abundance of reported bone marrow niche cell types and their combinations. *Blood*. 2020;136(20):2296-2307.

53. Méndez-Ferrer S, Lucas D, Battista M, Frenette PS. Haematopoietic stem cell release is regulated by circadian oscillations. *Nature*. 2008;452(7186):442-447.
54. Peled A, Petit I, Kollet O, et al. Dependence of human stem cell engraftment and repopulation of NOD/SCID mice on CXCR4. *Science*. 1999;283(5403):845-848.
55. Bonig H, Priestley GV, Nilsson LM, Jiang Y, Papayannopoulou T. PTX-sensitive signals in bone marrow homing of fetal and adult hematopoietic progenitor cells. *Blood*. 2004;104(8):2299-2306.
56. Greenbaum A, Hsu YMS, Day RB, et al. CXCL12 in early mesenchymal progenitors is required for haematopoietic stem-cell maintenance. *Nature*. 2013;495(7440):227-230.
57. Hou M, Andersson PO, Stockelberg D, Mellqvist UH, Ridell B, Wadenvik H. Plasma thrombopoietin levels in thrombocytopenic states: implication for a regulatory role of bone marrow megakaryocytes. *Br J Haematol*. 1998;101(3):420-424.
58. Guo L, Kapur R, Aslam R, et al. Antiplatelet antibody-induced thrombocytopenia does not correlate with megakaryocyte abnormalities in murine immune thrombocytopenia. *Scand J Immunol*. 2018;88(1):e12678.
59. Bujanover N, Goldstein O, Greenspan Y, et al. Identification of immune-activated hematopoietic stem cells. *Leukemia*. 2018;32(9):2016-2020.
60. Zhou BO, Yue R, Murphy MM, Peyer JG, Morrison SJ. Leptin-receptor-expressing mesenchymal stromal cells represent the main source of bone formed by adult bone marrow. *Cell Stem Cell*. 2014;15(2):154-168.
61. Tzeng YS, Li H, Kang YL, Chen WC, Cheng WC, Lai DM. Loss of Cxcl12/Sdf-1 in adult mice decreases the quiescent state of hematopoietic stem/progenitor cells and alters the pattern of hematopoietic regeneration after myelosuppression. *Blood*. 2011;117(2):429-439.
62. Nie Y, Han Y-C, Zou Y-R. CXCR4 is required for the quiescence of primitive hematopoietic cells. *J Exp Med*. 2008;205(4):777-783.
63. Crane GM, Jeffery E, Morrison SJ. Adult haematopoietic stem cell niches. *Nat Rev Immunol*. 2017;17(9):573-590.
64. Johns JL, Borjesson DL. Downregulation of CXCL12 signaling and altered hematopoietic stem and progenitor cell trafficking in a murine model of acute Anaplasma phagocytophilum infection. *Innate Immun*. 2012;18(3):418-428.
65. Wang X, Cho SY, Hu CS, Chen D, Roboz J, Hoffman R. C-X-C motif chemokine 12 influences the development of extramedullary hematopoiesis in the spleens of myelofibrosis patients. *Exp Hematol*. 2015;43(2):100-109.e1.
66. Decker M, Martinez-Morentin L, Wang G, et al. Leptin-receptor-expressing bone marrow stromal cells are myofibroblasts in primary myelofibrosis. *Nat Cell Biol*. 2017;19(6):677-688.
67. Bixel MG, Kusumbe AP, Ramasamy SK, et al. Flow dynamics and HSPC homing in bone marrow microvessels. *Cell Rep*. 2017;18(7):1804-1816.